



Active Control of Rotating Machinery Under Rotor-Stator Contact Conditions

Patrick S. Keogh^(✉), Chris Lusty, Nicola Y. Bailey, and Fawaz Saket

Department of Mechanical Engineering, University of Bath, Bath BA27AY, UK
p. s. keogh@bath. ac. uk

Abstract. A rotor spinning within an active magnetic bearing (AMB) system will normally be levitated and hence operate without rotor-stator contact. External disturbances and inherent unbalance may be compensated with appropriate control to keep rotor deviations within the clearance gap. However, AMBs have limited dynamic load capacity due to magnetic material field saturation. Hence overload conditions may result in rotor-stator contact. A touchdown bearing (TDB) and rotor landing sleeve are usually included to protect the expensive rotor, magnetic bearing and sensor components from damage. Once rotor-TDB contact has been made, rotor dynamic conditions may ensue resulting in persistent rotor bouncing or rubbing limit cycle responses. Prolonged exposure to these severe dynamics will cause TDB degradation and require regular replacement. If possible, a clear aim should be to restore contact-free levitation through available control capability in an efficient manner. This paper is used to guide the control options that are available to restore contact-free levitation. The use of AMB control is appropriate if the required control forces are within saturation limits. It is also possible to actuate TDBs and destabilize persistent rotor dynamic contact conditions. For example, piezo-based actuation offers larger control forces than those from magnetic bearing systems. Hybrid control action involving both types of actuation system has the greatest potential for completely robust restoration of contact-free levitation.

Keywords: Magnetic bearings · Touchdown bearings · Contact-free levitation

1 Introduction

It is a current focus for the designers and manufacturers of active magnetic bearing (AMB) systems to give significant attention to the associated touchdown bearing (TDB) systems. The TDB is included to prevent damage to expensive rotor and stator components and to ensure that run-downs are safe. The sacrificial components are the replaceable TDB and rotor landing sleeve. During rotor-TDB contact, the TDB may be stressed mechanically and thermally, reducing TDB residual life significantly. It is therefore beneficial for the TDB to minimize contact periods to reduce losses of machine output and downtime.

Loss of levitation that causes rotor drop is the most severe duty experienced by a TDB [1, 2]. Larger scale drop tests are presented in [3–6]. Simulation of rotor drop includes the nonlinear study of [7]. Research in this area has continued to bring out the

finer details of the rotor dynamic and TDB responses [8–10]. Recently, significant further activity has also followed [11–20].

If a rotor/AMB system is still able to operate normally under closed loop control, the following scenarios may occur leading to rotor/TDB contact:

- (a) Feedback signal disturbances may lead to significant momentary rotor excursions.
- (b) Base accelerations or shock inputs may overload the AMBs, hence limiting rotor dynamic control.
- (c) Contact induced dynamics may become persistent or changed so much that the AMB closed loop control is unstable.

One course of action is to apply additional AMB control action to restore contact-free levitation [21, 22]. Alternatively, the TDB may be changed from being a passive component to an active component. This was achieved in [23–26].

Given the previous studies, it is useful to have a greater understanding of rotor contact dynamics. This would aid the design of control strategies that are able to restore contact-free levitation from a persistent condition of rotor-TDB contact. A distinction is made from standard controllers that are designed based on a contact-free rotor dynamic plant model. The reason is that under persistent contact, the rotor dynamic plant changes, hence the standard controllers may not respond appropriately or may induce rotor dynamic instability unintentionally. In order to ascertain the principles required for the restoration of contact-free levitation, the issues are assessed using an analytical model of a simple rotor supported in an AMB/TDB system. Conditions to destabilize persistent rub contact responses are derived. Simulations are then used to demonstrate how feedforward control of AMBs and TDBs may be used effectively. Feedforward AMB action may be appropriate if dynamic load capacity is available. Otherwise, feedforward TDB motions may be able to induce the rotor away from persistent contact.

2 Modeling of Rotor/TDB Contact

Figure 1 shows a simplified schematic of a section of rotor within an active magnetic bearing (AMB), which has made contact with a portion of a touchdown bearing (TDB). The TDB may have some degree of radial stiffness and damping in its mounting arrangement. Under standard proportional-integral-derivative (PID) control, the linearized AMB radial characteristics are isotropic and may be represented by stiffness and damping from the magnetic center. The purpose of the TDB is to prevent contact between the rotor and AMB magnetic poles, hence the rotor-AMB radial gap is designed to be less than the rotor-TDB radial gap. In practice, the AMB may have a significant axial dimension and the TDB is located adjacent to the AMB. Hence the TDB in Fig. 1 will be generally axially offset from the AMB. This non-collocation should be taken into account in the system design so that rotor tilt through the AMB, arising from conical and flexible rotor modes, does not allow rotor-AMB contact.

In the following section that considers an analytical approach to determine rotor/TDB rub responses, the AMB and TDB are considered to be axially aligned and the TDB rigidly mounted. This is an idealized representation. In Sect. 3.5, simulated

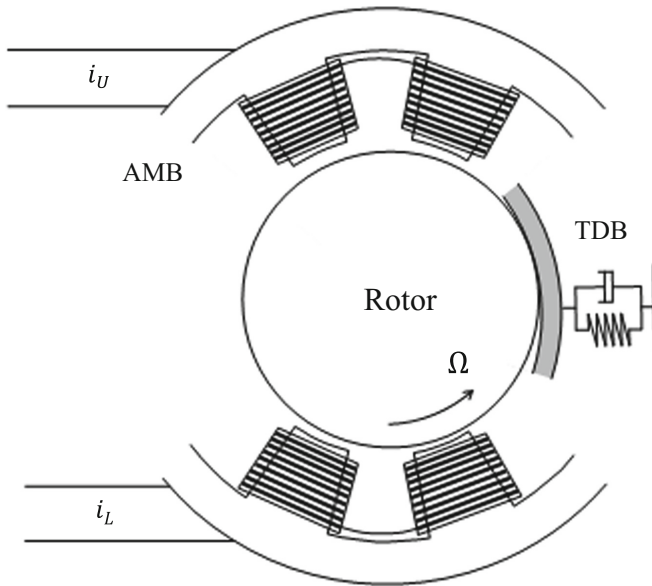


Fig. 1. Simulation of a rotor making contact with a touchdown bearing (TDB) within a functional AMB.

results are presented under compliant TDB mounting and it will be demonstrated that the analytical representations provide insight into the rotor rub response behavior. Relevant system parameters are shown in Table 1.

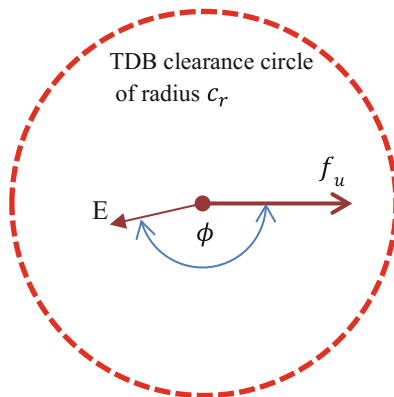


Fig. 2. Steady forward synchronous orbit representation of Eq. (4) viewed in a (u, v) rotating frame. The length of the displacement to E is r_E .

2.1 Synchronous Rotor Response

In this case the rotor is considered to be a simple unbalanced mass, m , that can rotate and translate in fixed axis x and y directions. In the following, E will denote the case of rotor motion that excludes rotor-TDB contact, while C will denote rotor motion with rotor-TDB contact. The orbit motions may be viewed in a fixed Cartesian (x, y) system or a synchronously rotating (u, v) system. The relation between the systems is

$$z = x + iy, \quad w = u + iv = ze^{-i\Omega t} \quad (1)$$

where Ω is the rotational speed. The AMB radial stiffness and damping characteristics may be specified through a natural frequency ω_n and damping ratio ξ so that

$$\ddot{z}_{E,C} + 2\xi\omega_n\dot{z}_{E,C} + \omega_n^2 z_{E,C} = \frac{f_u}{m} e^{i\Omega t} - \frac{f_c}{m} (1 + i\mu) \frac{z_C}{c_r} \quad (2)$$

or

$$\ddot{w}_{E,C} + (2\xi\omega_n + 2i\Omega)\dot{w}_{E,C} + (\omega_n^2 - \Omega^2 + 2i\xi\omega_n\Omega)w_{E,C} = \frac{f_u}{m} - \frac{f_c}{m} (1 + i\mu) \frac{w_C}{c_r} \quad (3)$$

where the subscripts E and C correspond with the orbit motions E and C, respectively. Also, c_r is the rotor-TDB radial clearance, f_u is the rotor unbalance amplitude, f_c is the normal contact force, and μ is the coefficient of friction between the rotor and TDB. Obviously, for orbit motions E, $f_c = 0$ always.

Under steady state forward synchronous motions, the non-contacting orbit corresponds with

$$w_E = r_E e^{-i\phi} = \frac{f_u}{m(\omega_n^2 - \Omega^2 + 2i\xi\omega_n\Omega)} \quad (4)$$

The force displacement relation of Eq. (4) may be represented in the (u, v) plane as shown in Fig. 2.

In the case of a steady forward synchronous rub orbit, $w_C = c_r e^{-i\psi}$ where ψ is some phase angle, it follows from Eq. (3) that

$$(\omega_n^2 - \Omega^2 + 2i\xi\omega_n\Omega)c_r e^{-i\psi} = \frac{f_u}{m} - \frac{f_c}{m} (1 + i\mu) e^{-i\psi} \quad (5)$$

With the inclusion of the contact components of force (normal and tangential friction), a resultant synchronous force of amplitude f_s must exist to drive the orbit at C in the same way that f_u drives the orbit at E (see Fig. 3). It follows from Eqs. (4) and (5) and the force equilibrium shown in Fig. 3 that

$$\frac{f_u c_r}{m r_E} e^{i(\phi-\psi)} = \frac{f_u}{m} - \frac{f_c}{m} (1 + i\mu) e^{-i\psi} = \frac{f_s}{m} e^{i(\phi-\psi)} \quad (6)$$

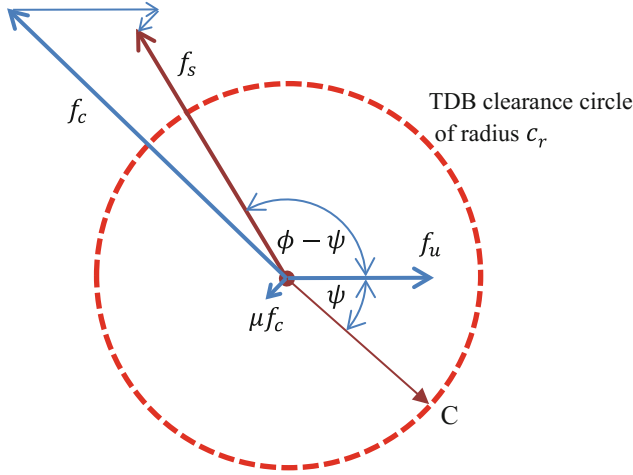


Fig. 3. Steady forward synchronous rub orbit, C, viewed in a (u, v) rotating frame. In order to drive the orbit to C, a synchronously rotating force of amplitude f_s must exist with a phase lead of ϕ on the vector to C.

Hence,

$$f_s = f_u \frac{c_r}{r_E} \quad (7)$$

and

$$f_c = \frac{f_u}{(1 + i\mu)} \left(e^{i\psi} - \frac{c_r}{r_E} e^{i\phi} \right) \quad (8)$$

Although the force expression in Eq. (8) is complex, if it is to be a genuine physical force amplitude arising from contact, then

$$\left. \begin{aligned} \text{Im}f_c &= \text{Im} \left(\frac{f_u}{(1 + i\mu)} \left(e^{i\psi} - \frac{c_r}{r_E} e^{i\phi} \right) \right) = 0 \\ \text{Re}f_c &= \text{Re} \left(\frac{f_u}{(1 + i\mu)} \left(e^{i\psi} - \frac{c_r}{r_E} e^{i\phi} \right) \right) > 0 \end{aligned} \right\} \quad (9)$$

In general, ψ should be varied until the conditions of Eq. (9) are satisfied to determine the rub orbit. Ultimately, in contrast with Eq. (4), the rubbing contact satisfies

$$w_C = c_r e^{-i\psi} = \frac{f_s e^{i(\phi - \psi)}}{m(\omega_n^2 - \Omega^2 + 2i\zeta\omega_n\Omega)} \quad (10)$$

3 Control for Contact-Free Levitation

3.1 AMB Synchronous Forcing

If AMB functionality exists, an obvious procedure to restore contact-free levitation is to apply AMB synchronous forcing at some phase angle α :

$$f_{AMB} = f_A e^{i\alpha} \quad (11)$$

For the simple rigid disk analysis considered in Sect. 2, this is simply superimposed onto the synchronous unbalance force, f_u .

3.2 Active TDB Synchronous Motion

Consider the TDB to be actuated under sufficiently strong control such that demand motions may be imposed. Suppose then that forward synchronous whirl motion of the TDB is enabled in the form

$$w_B = r_B e^{i\beta} \quad (12)$$

where β is some phase angle. When viewed in the (u, v) plane, this corresponds to a shift of the rotor-TDB clearance circle at an angle β relative to the unbalance vector. It is therefore of interest to evaluate the relative rotor to TDB displacement

$$w_{CB} = w_C - w_B \quad (13)$$

Equation (3) should then be modified to

$$\begin{aligned} \ddot{w}_{CB} + (2\zeta\omega_n + 2i\Omega)\dot{w}_{CB} + (\omega_n^2 - \Omega^2 + 2i\zeta\omega_n\Omega)w_{CB} \\ = \frac{f_u}{m} - \frac{f_c}{m} (1 + i\mu) \frac{w_{CB}}{c_r} - (\omega_n^2 - \Omega^2 + 2i\zeta\omega_n\Omega)w_B \\ = \frac{f_u}{m} \left(1 - \frac{r_B}{r_E} e^{i(\beta + \phi)} \right) - \frac{f_c}{m} (1 + i\mu) \frac{w_{CB}}{c_r} \end{aligned} \quad (14)$$

3.3 Criteria for Contact to Fail to Exist

Suppose that AMB synchronous forcing of Eq. (11) is applied simultaneously with the TDB motion of Eq. (12). Following through the analysis of Sect. 2.1, steady synchronous forward rubbing will exist if

$$\begin{aligned} \text{Im}f_c = \text{Im} \left(\frac{1}{(1+i\mu)} \left\{ f_A e^{i\alpha} + f_u \left(1 - \frac{r_B}{r_E} e^{i(\beta + \phi)} \right) \right\} \left(e^{i\psi} - \frac{c_r}{r_E} e^{i\phi} \right) \right) = 0 \\ \text{Re}f_c = \text{Re} \left(\frac{1}{(1+i\mu)} \left\{ f_A e^{i\alpha} + f_u \left(1 - \frac{r_B}{r_E} e^{i(\beta + \phi)} \right) \right\} \left(e^{i\psi} - \frac{c_r}{r_E} e^{i\phi} \right) \right) > 0 \end{aligned} \quad (15)$$

It follows that by violating these conditions for all cases of ψ , then no steady state rub condition is possible.

3.4 Practicalities for Contact Determination

If a control strategy to restore contact-free levitation is to be implemented, it would be useful to identify the following data as occurring in Eq. (15):

- (a) The unbalance amplitude, f_A , and a zero phase reference for the unbalance vector.
- (b) The contact-free orbit radius, r_E , and its phase, ϕ , relative to the unbalance vector.
- (c) The coefficient of friction, μ .

Note that the conditions of Eq. (15) have been derived assuming a zero phase reference for the unbalance. The required data could be obtained through periodic monitoring and updating using the AMB control system. If done, then this knowledge may be used to select appropriate control for contact-free restoration either through the AMB alone, the TDB alone or as a combination of both.

It would also be useful to have some trigger system to indicate when contact has occurred. This could be achieved using stator-mounted accelerometers to detect responses to contact force transmission. Displacement transducers that provide signals for feedback control of AMBs may also be used, though care is required to decide between a large non-contacting orbit and a real rub orbit, since there are significant phase differences between the two cases. Transducer systems that respond directly to contact forces may also have potential [27].

The results in the previous sections have been derived under steady state assumptions. In reality, the motion from a contact-free orbit E to a contact orbit C will involve some intervening transient motion involving possible bounce-like behavior. To assess the effectiveness of the analytical derivations, a series of dynamic simulations now follow.

3.5 Simulated Motions

Simulations were undertaken with a resiliently mounted TDB model (Fig. 1). Parameter values used are shown in Table 1.

Table 1. Parameters used for simulations.

Parameter	Value
k_B (TDB radial support stiffness)	6×10^6 N/m
c_B (TDB radial support damping)	2500 Ns/m
m_B (TDB mass)	0.18 kg
m (rotor mass)	4.25 kg
μ (coefficient of friction between rotor and TDB)	0.05
TDB inner radius	15 mm
TDB inner race material	Steel
Rotor material	Steel
AMB magnetic gap	0.8 mm
AMB under PD control rotor natural frequency	638 rad/s
AMB under PD control rotor damping ratio	0.086
Ω (rotor speed)	1000 rad/s

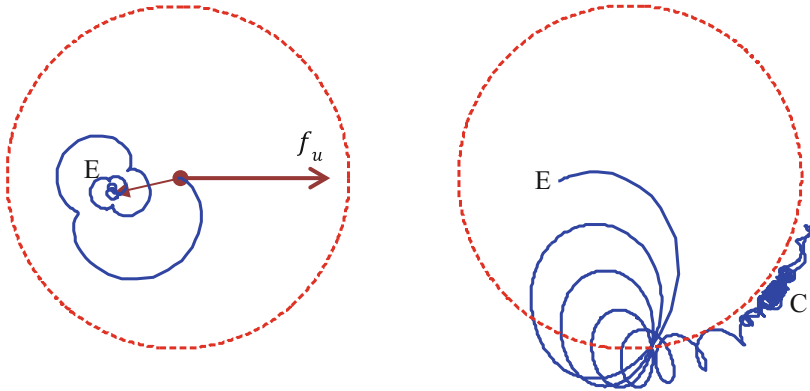


Fig. 4. Synchronous (u, v) rotating frame views. The left figure shows the effect of a step change of unbalance, which leads to the steady state position E after transient motion. The right figure shows the effect of a subsequent velocity input to the rotor, leading to the steady state contact response at C after transient motion that involves bouncing contact.

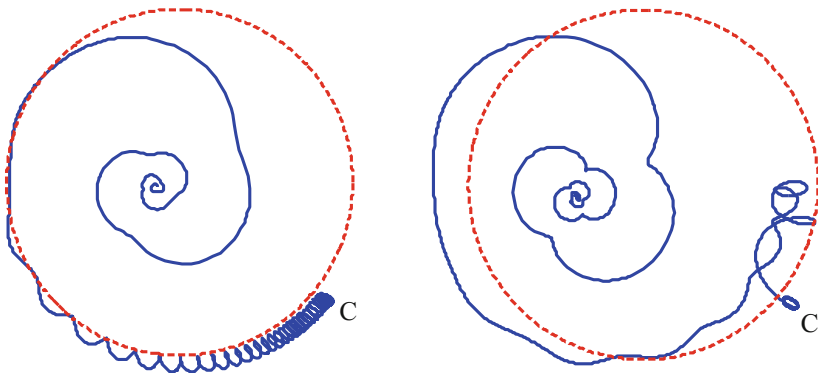


Fig. 5. Synchronous (u, v) rotating frame views. The left figure shows the effect of applying a ramped force at 180° phase to the unbalance, which leads to the restoration of contact-free levitation after transient motion. The right figure shows the effect of a synchronous TDB motion with -4.5° phase, which leads to the restoration of contact-free levitation after transient motion.

A Hertzian model was used to represent the normal contact stresses between the rotor and TDB. Starting from a rotor spinning precisely at the AMB magnetic center, a step change of unbalance (425 N) was applied. The left plot of Fig. 4 shows the transient response of the rotor, which does not involve any TDB contact, to the steady orbit at E. A sudden velocity input of 0.3 m/s (horizontal) was then imposed while the unbalance remained unchanged. The right plot of Fig. 4 shows that the rotor interacts with the TDB, undergoing several bounces, before settling on the rub orbit C. The red dashed clearance circles correspond with the centered TDB position (undeflected). The appearance of the rub orbit C lying outside the clearance circle indicates that the TDB has deflected on its resilient mount.

It is interesting to note that the simulated results of Fig. 4 show similar orbit positions for E and C from the analytical model results of Figs. 2 and 3. In the simulated case of Fig. 4, orbit C lies outside the nominal clearance circle of the TDB, a consequence of the fact that the compliantly mounted TDB experiences whirling with the contacting rotor. In effect, the final steady rub orbit would be similar to that of a rigidly mounted TDB having an appropriately larger rotor to TDB radial clearance.

Feedforward control was then applied as guided by the conditions of Eq. (15). The left plot of Fig. 5 shows how feedforward AMB control in the form of a ramped synchronous force was able to destabilize the rotor rub orbit at C. The right plot of Fig. 5 shows how a step change of synchronous TDB orbit motion was able to achieve a similar result.

4 Conclusions

Analytical expressions have been used to show how synchronous forward rubbing may coexist with a contact-free forward whirl under the same rotor dynamic unbalance. These bi-stable responses are differentiated by the relative orbit sizes and significant phase differences. The orbits were evaluated in a synchronously rotating reference frame in which the usual circular whirl orbits are represented as stationary points. A complex representation was used to evaluate contact forces and conditions were established to define whether a rub orbit was able to exist. These conditions were extended to include contributions from feedforward AMB synchronous forcing and feedforward TDB synchronous orbits. This enabled deductions to be made on how these feedforward motions could be used to destabilize a rotor-TDB contact orbit.

Simulations of rotor to TDB contact were also undertaken and these confirmed that the analytical results guide understanding of the nonlinear dynamics and the final rub orbit. The simulations were also extended to demonstrate how the feedforward control was also effective with a resiliently mounted TDB and the presence of significant transient motion in the transitions between steady state orbits.

References

1. Bartha, A.R.: Dry friction induced backward whirl: theory and experiment. In: Proceedings of the 5th IFToMM Conference on Rotor Dynamics, Darmstadt, Germany (1988)
2. Fumagalli, M., Varadi, P., Schweitzer, G.: Impact dynamics of high speed rotors in retainer bearings and measurement concepts. In: Proceedings of the 4th International Symposium on Magnetic Bearings (ISMB4), Zurich, Switzerland (1994)
3. Schmied, J., Pradetto, J.C.: Behavior of a one ton rotor being dropped into auxiliary bearings. In: Proceedings of the 3rd International Symposium on Magnetic Bearings (ISMB3), Alexandria, USA (1992)
4. Kirk, R.G., Ishii, T.: Transient response drop analysis of rotors following magnetic bearing power outage. In: Proceedings of the MAG 1993, Alexandria, USA (1993)
5. Kirk, R.G., Swanson, E.E., Kavarana, F.H., Wang, X.: Rotor drop test stand for AMB rotating machinery, part 1: description of test stand and initial results. In: Proceedings of the 4th International Symposium on Magnetic Bearings (ISMB4), Zurich, Switzerland (1994)

6. Swanson, E.E., Kirk, R.G., Wang, J.: AMB rotor drop initial transient on ball and solid bearings. In: Proceedings of the MAG 1995, Alexandria, USA (1995)
7. Foiles, W.C., Allaire, P.E.: Nonlinear transient modeling of active magnetic bearing rotors during rotor drop on auxiliary bearings. In: Proceedings of MAG 1997, Alexandria, USA, pp. 154–163 (1997)
8. Sun, G., Palazzolo, A.B., Provenza, A., Montague, G.: Detailed ball bearing model for magnetic suspension auxiliary service. *J. Sound Vib.* **269**(3), 933–963 (2004)
9. Helfert, M., Ernst, M., Nordmann, R., Aeschlimann, B.: High-speed video analysis of rotor-retainer-bearing-contacts due to failure of active magnetic bearings. In: Proceedings of the 10th International Symposium on Magnetic Bearings, Martigny, Switzerland (2006)
10. Hawkins, L., Filatov, A., Imani, S., Prosser, D.: Test results and analytical predictions for rotor drop testing of an active magnetic bearing expander/generator. *Trans. ASME J. Eng. Gas Turbines Power* **129**, 522–529 (2007)
11. Janse van Rensburg, J.J., van Schoor, G., van Vuuren, P.: The characterization of the severity of rotor delevitation events—a parametric study. In: Proceedings of the 13th International Symposium on Magnetic Bearings (ISMB 2013), Arlington, USA (2012)
12. Janse van Rensburg, J.J., Vanek, C., Worlitz, F.: Backup bearing modelling for turbo machines with high axial and radial loads. In: Proceedings of the 14th International Symposium on Magnetic Bearings (ISMB 2014), Linz, Austria (2014)
13. Collins, T., Masala, A., Shultz, R., Guo, Z.: Numerical and experimental results of auxiliary bearings testing on a high speed test rig. In: Proceedings of the 14th International Symposium on Magnetic Bearings (ISMB 2014), Linz, Austria (2014)
14. Denk, J., Köhler, B.-E., Siegle, G., Siebke, P.: Landing tests with a 6300 rpm, 9 t AMB rotor in rolling element back-up bearings. In: Proceedings of the 14th International Symposium on Magnetic Bearings (ISMB 2014), Linz, Austria (2014)
15. Siebke, P., Golbach, H.: A novel rolling element back-up bearing for a 9 t rotor application. In: Proceedings of the 14th International Symposium on Magnetic Bearings (ISMB 2014), Linz, Austria (2014)
16. Siegl, G., Tzianetopoulou, T., Denk, J.: Simulation and experimental validation of a 9 ton AMB rotor landing in rolling element back-up bearings. In: Proceedings of the 14th International Symposium on Magnetic Bearings (ISMB 2014) (2014). Linz, Austria and the J. Jpn. Soc. Mech. Eng. Article ID: 15-00136 (2016)
17. Yang, G., Shi, Z., Liu, X., Zhao, J.: Research and experiment of auxiliary bearings with no lubrication for helium blower of HTR-10. In: Proceedings of the 14th International Symposium on Magnetic Bearings (ISMB 2014), Linz, Austria (2014)
18. Lahriri, S., Santos, I.F.: Theoretical modelling, analysis and validation of the shaft motion and dynamic forces during rotor–stator contact. *J. Sound Vib.* **332**, 6359–6376 (2013)
19. Lee, J.L., Palazzolo, A.: Catcher bearing life prediction using a rainflow counting approach. *Trans. ASME J. Tribol.* **134**(3), 031101 (2012)
20. Anders, J., Leslie, P., Stacke, M.L.-E.: Rotor drop simulations and validation with focus on internal contact mechanisms of hybrid ball bearings. Paper GT2013-95816, ASME/IGTI Turbo Expo, San Antonio, USA (2013)
21. Keogh, P.S., Cole, M.O.T.: Rotor vibration with auxiliary bearing contact in magnetic bearing systems, Part I: synchronous dynamics. In: Proceedings of the Institution of Mechanical Engineers, Part C, vol. 217, pp. 377–392 (2003)
22. Cole, M.O.T., Keogh, P.S.: Asynchronous periodic contact modes for rotor vibration within an annular clearance. In: Proceedings of the Institution of Mechanical Engineers, Part C, vol. 217, pp. 1101–1115 (2003)

23. Ulbrich, H., Ginzinger, L.: Stabilization of a rubbing rotor using a robust feedback control, Paper-ID: 306. In: Proceedings of the 7th IFToMM Conference on Rotor Dynamics, Vienna, Austria (2006)
24. Cade, I.S., Sahinkaya, M.N., Burrows, C.R., Keogh, P.S.: On the design of an active auxiliary bearing for rotor/magnetic bearing systems. In: Proceedings of the 11th International Symposium on Magnetic Bearings (ISMB 2011), Nara, Japan (2008)
25. Keogh, P.S., Sahinkaya, M.N., Burrows, C.R., Cade, I.S.: Rotor/auxiliary bearing dynamic contact modes in magnetic bearing systems. In: Proceedings of the 11th International Symposium on Magnetic Bearings (ISMB 2011), Nara, Japan (2008)
26. Li, P., Sahinkaya, M.N., Keogh, P.S.: Active touchdown bearing control for recovery of contact-free rotor levitation in AMB systems. In: Proceedings of the 14th International Symposium on Magnetic Bearings (ISMB 2014), Linz, Austria (2014)
27. Saket, F.Y., Sahinkaya, M.N., Keogh, P.S.: Experimental assessment of touchdown bearing contact forces in magnetic bearing systems. In: 9th IFToMM International Conference on Rotor Dynamics, Milan, Italy (2014)